



Base-state dependence of parameter sensitivity for the Twomey effect in a perturbed parameter ensemble

Sophie Wynn¹, Duncan Watson-Parris^{1,2}, Brandon M. Duran¹, Johannes Mülmenstädt³

5

¹Scripps Institution of Oceanography, University of California San Diego, La Jolla, CA, USA

²Halcioğlu Data Science Institute, University of California San Diego, La Jolla, CA, USA

³Atmospheric, Climate and Earth Sciences Division, Pacific Northwest National Laboratory, Richland, WA, USA

10 *Correspondence to:* Sophie Wynn (srwynn@ucsd.edu)

15

20



25 Abstract

A major source of uncertainty in the effective radiative forcing due to aerosol-cloud interactions (ERF_{aci}) arises from parameters that represent unresolved sub-grid-scale processes in global climate models. Constraining parametric uncertainty requires identifying parameters driving the largest spread in ERF_{aci}. Perturbed parameter ensembles (PPE) address this by systematically varying parameters related to aerosol emission, cloud microphysics, and associated small-scale processes. We perform a global sensitivity analysis of the three components of ERF_{aci} from liquid clouds, the Twomey effect, liquid water path (LWP), and cloud fraction (CF) adjustments, in a PPE with and without constraining to the model's present-day base state. Under uniform prior sampling, autoconversion parameters unrelated to aerosol activation counterintuitively dominate the Twomey effect. Only after constraining the base state are aerosol emission and activation parameters revealed as controlling parameters for the Twomey effect. The apparent control of autoconversion parameters over the Twomey effect arises because these parameters control the cloud base state, which in turn affects the strength of the Twomey effect. The dominant parameters for LWP and CF adjustments remain related to autoconversion before and after the constraint. Constraining to the base state is therefore essential to inferring the correct parameters and processes controlling the model's climate responses.

40 1 Introduction

Anthropogenic perturbations in greenhouse gases and aerosols emission have generally warmed the climate. Work to constrain the estimate of effective radiative forcing is primarily focused on reducing the large uncertainty associated with aerosols interactions with clouds which partially offsets this warming (Watson-Parris 2025, Bellouin et al., 2020). Part of this large uncertainty in forcing comes from representation of aerosol-cloud interactions (ACI) in global climate models (GCMs) (Seinfeld et al., 2016; Mülmenstädt and Feingold 2018). GCMs utilize parameterizations to represent processes related to ACI including aerosol emission, cloud microphysics, radiation, and convection. These small-scale processes are not resolved due to the typical model grid size resolution of 1° longitude × 1° latitude and are represented using parameterizations derived from a combination of theory, higher resolution models and observations. Thus, these simplifications introduce uncertainties over and above the inherent structural uncertainties of the model (Regayre et al., 2018, Morrison et al., 2020).

The radiative effects of ACI arise from two components, an instantaneous cloud brightening (Twomey) radiative forcing and secondary adjustments that can either amplify or offset this initial forcing (Twomey, 1977). The Twomey effect occurs when anthropogenic aerosols serve as additional cloud condensation nuclei (CCN) and, assuming a fixed amount of cloud liquid water, leads to an increase in the cloud droplet number concentration (CDNC), reducing the effective radius of the cloud droplets (r_e). This increases the reflected shortwave radiation of the cloud and causes a cooling effect. Macrophysically, this



increase in CDNC can either lead to negative or positive adjustment to forcing. These adjustments can manifest as a change in the liquid water path (LWP) or cloud fraction (CF). Precipitation suppression is one pathway where the smaller droplets lead to an increase in the cloud's LWP and lifetime, causing a more negative ERF_{aci} (cooling) (Albrecht, 1989; J. Quaas 60 2009). However, under different conditions, smaller cloud droplets can lead to enhanced above cloud evaporative cooling and an enhanced entrainment of dry air at cloud tops causing a decrease in LWP and cloud lifetime and leading to a less negative ERF_{aci} (warming) (Ackerman et al., 2004; Bretherton et al., 2007; J. Quaas 2009; Chen et al. 2014). These competing adjustments make the net ERF_{aci} highly uncertain.

65 Studies that aim to understand ACI in GCMs increasingly use a perturbed parameter ensemble (PPE) to understand these competing effects and their relative contributions (Lee et al., 2011, 2013; Eidhammer et al., 2024; Gettelman et al., 2024; Song et al., 2024; Mikkelsen et al., 2025; Yang et al., 2025; Bhatti et al., 2026). In PPEs, parameters related to ACIs are varied throughout a large ensemble to produce a wide range of aerosol forcing estimates. Output from PPEs is used to explore parametric uncertainty, constrain aerosol forcing, and further understand key processes related to ACI in GCMs. 70 Elsaesser et al. (2025) develop a calibrated physics ensemble (CPE) for the NASA Model-E and found that parameter-output relationships differ when parameter values are constrained by observations compared to the initial ensemble. In particular, they found that some cloud parameters that appeared unimportant in their initial PPE became important once calibrated to observations, while other parameters showed reduced influence. It is important to note that this is not only because the relative importance of key parameters are reduced, but also because of the non-linearities in the cloud system where 75 parameter importances can vary across regions of parameter space. Given the non-linearities described above, such state dependence in the parameter sensitivities should also be present in aerosol processes related to ACI, but we are not aware of any previous studies that have explicitly quantified this.

Our study uses a new PPE of the Community Atmosphere Model, version 6 (CAM6; Duran et al 2025a), which includes 80 output for the Duran et al., (2025b) MODIS cloud radiative kernel method to decompose short wave (SW) ERF_{aci} from liquid-topped clouds into the Twomey effect, LWP and CF adjustments. We investigate the parameter sensitivities of the three components of SW ERF_{aci} while accounting for the model's present-day (PD) cloud base state for liquid clouds. To do so, we restrict our analysis to parameter combinations that produce a climate defined by global mean LWP, ice water path (IWP), top of atmosphere (TOA) net SW flux, and the liquid CF of the CAM6 ensemble member with default parameter 85 values ("control" ensemble member). We argue that accounting for the PD model base state is essential when exploring parametric uncertainty in a GCM. As we show in the following, allowing unrealistic cloud properties can distort the assessment of parameter sensitivity, leading to incorrect conclusions about parameter importance.



2 Results

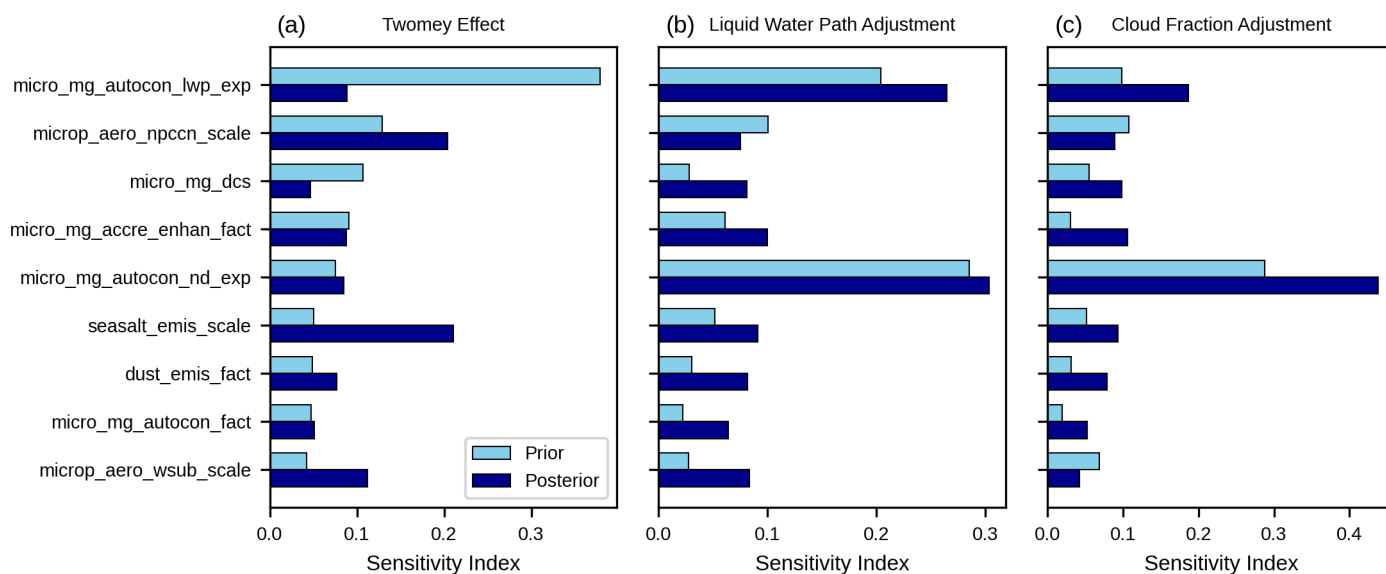
90 Figure 1 shows a global sensitivity analysis (Pianosi and Wagener, 2015) for each of the components of SW ERF_{aci} from liquid clouds contributed by the global mean climatological Twomey effect, LWP adjustment and CF adjustment. A high sensitivity index indicates a parameter whose variation produces large changes in the output distribution. The Twomey effect exhibits a strong dependence on the model base state, with the dominant parameters differ markedly between the prior (uniform sampling) and posterior distributions. Under prior sampling, the most influential parameter is in the autoconversion scheme and represents the exponent on the cloud water mass mixing ratio (*micro_mg_autocon_lwp_exp*; Khairoutdinov and Kogan, 2000; KK2000). Variations in this parameter greatly impact the amount of cooling from the Twomey effect. The 95 second most influential parameter is the scaling of aerosol activation to cloud droplet number (*microp_aero_npccn_scale*), followed by the size threshold for ice-to-snow conversion (*micro_mg_dcs*). Other parameters that exhibit influence on the Twomey effect are related to the warm rain process (*micro_mg_autcon_nd_exp*, *micro_mg_accre_enhan_fact*) and sea salt emissions (*seasalt_emis_scale*).

100 The posterior distribution is formed by retaining only parameter combinations from the prior that reproduce the PD global mean base state of the default model simulation. Global mean LWP, IWP, liquid CF, and TOA net SW flux were selected as constraints to represent the model's base state. Once constrained to the base state, the dominant parameters for the Twomey effect change, the most dominant parameter in the prior (*micro_mg_autocon_lwp_exp*) massively decreases in importance and the most sensitive parameters emerge as related to emission and activation of aerosols. These parameters include 105 *seasalt_emis_scale*, *microp_aero_npccn_scale*, as well as the parameter controlling the scaling of sub grid cell velocity for liquid activation of aerosols (*microp_aero_wsub_scale*). The dominant parameters for both the LWP and the CF adjustment do not change when we constrain to the base state, both parameters are exponents in the KK2000 autoconversion parameterization (*micro_mg_autcon_nd_exp*, *micro_mg_autcon_lwp_exp*) and remain the most important for both adjustments.

110



Parameter Sensitivity for Global Mean ERFaci Liquid Cloud Decomposition



115 **Figure 1. Histograms of parameter sensitivity indices for the liquid cloud decomposed SW ERFaci forcing. Light blue represents the sensitivity of each parameter when sampling from the uniform prior distribution. Dark blue represents the sensitivity of each parameter when sampling from the posterior distribution that represents the model base state. Only the 9 most influential parameters are shown.**

120 Figure 2 shows which parameters are most important locally for the Twomey effect. The Twomey effect is strongest in areas of high pollution such as Southeast Asia, and Eastern North America, but is also important in stratocumulus regions such as the Southeast Pacific and Southeast Atlantic. Prior inputs show both dominant parameters to be members of the autoconversion scheme for warm rain and snow. The posterior distribution reveals the parametric sensitivity of the Twomey effect when the base state is fixed. The dominant parameters show a clear regime-like geographic structure. Over land and in regions of high

125 pollution, the dominant parameter is *microp_aero_wsub_scale*. Increasing this parameter activates a greater fraction of available aerosols as CCN by increasing updraft speeds, which produces more numerous but smaller cloud droplets, amplifying the Twomey effect. In coastal regions, *microp_aero_npccn_scale* is dominant. In the central North Pacific *seasalt_emis_scale* emerges as the most dominant parameter, highlighting the importance of natural emissions in remote environments. *Micro_mg_autcon_lwp_exp* remains dominant over the Southeast Pacific, where lower anthropogenic aerosol loading reduces

130 sensitivity to activation processes, leaving the background cloud liquid water state as the primary control on the Twomey effect. These regional contrasts distinguish updraft-limited polluted regimes, where aerosol activation is the limiting factor,

<https://doi.org/10.5194/egusphere-2026-2811>

Preprint. Discussion started: 19 June 2026

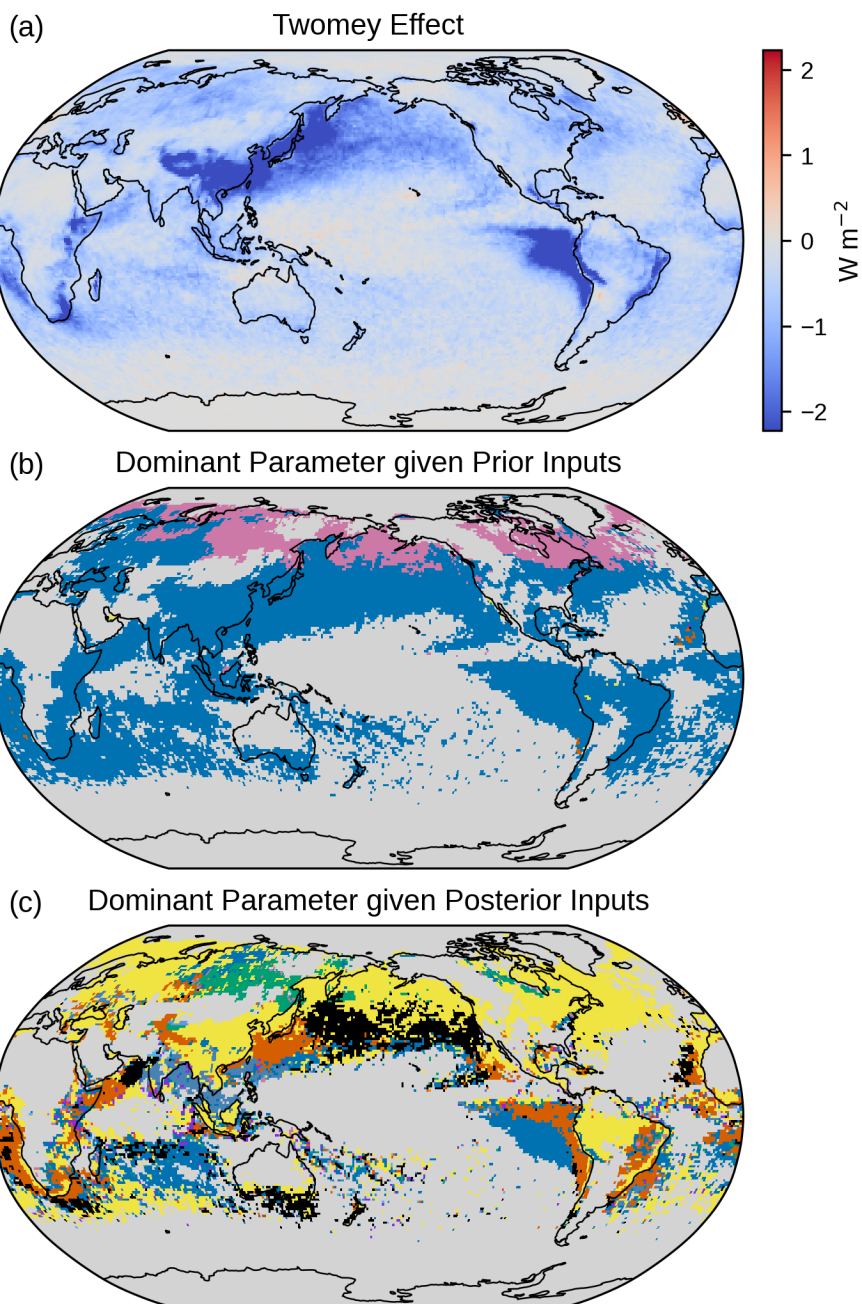
© Author(s) 2026. CC BY 4.0 License.



from aerosol-limited pristine regimes, where the background cloud state and natural emissions govern susceptibility to aerosol perturbations.



Local Twomey Effect Sensitivity



Parameters		
■ micro_mg_accre_enhan_fact	■ micro_mg_dcs	■ microp_aero_wsub_min
■ micro_mg_autocon_fact	■ micro_mg_vtrmi_factor	■ microp_aero_wsub_scale
■ micro_mg_autocon_lwp_exp	■ seasalt_emis_scale	■ microp_aero_wsubi_scale
■ micro_mg_autocon_nd_exp	■ microp_aero_npccn_scale	■ dust_emis_fact
■ micro_mg_berg_eff_factor		



140

Figure 2. Parameter sensitivity of the climatological mean liquid cloud Twomey effect resolved spatially. (a) The Twomey effect ($W m^{-2}$) for the base state default ensemble member. (b, c) The dominant parameter at each grid cell under the prior and posterior input distributions, respectively. The dominant parameter is identified as the one with the highest sensitivity index at each grid cell. In b and c only grid cells where the local Twomey effect magnitude exceeds 1.5 times the global median Twomey effect forcing are shown; all other regions are masked in grey.

3 Discussion

145

150

155

160

165

Our analysis uncovers the parameter sensitivities for the Twomey effect and macrophysical cloud adjustments for liquid clouds in CAM6. The Twomey effect exhibits the greatest dependence on base cloud state, as the most dominant parameter *micro_mg_autcon_lwp_exp*, decreases in sensitivity by 77% when the base state is constrained. For the Twomey effect, parameters related to aerosol emission and updraft activation are shown to be the most important when constrained to a realistic state of the model. *Micro_mg_autcon_lwp_exp*, which controls the condensate retention capacity of the clouds, is a false positive as it largely controls the background cloud state and adjustment behaviour. There is robust evidence that the present-day cloud base state can be a key determinant of the total ERF_{aci} (Douglas and L'Ecuyer 2019, Mülmenstädt et al., 2020, Wall et al., 2022, Song et al., 2024). Uniform sampling obscures the true sensitivity of the processes of interest by instead capturing sensitivity to the climate state and permits sampling of unrealistic climate scenarios. As an extreme example, in an environment with no clouds, increasing aerosol emission and activation would not lead to any cloud brightening via the Twomey effect. Our analysis also shows that accounting for ice water path is important for understanding liquid cloud behavior in models: without controlling for IWP, the parameter that governs the ice-to-snow conversion process (*microp_mg_dcs*) appeared to be the most important parameter for the Twomey effect, likely because ice clouds can obscure low-level liquid clouds. Through fixing PD IWP, *microp_mg_dcs* becomes much less important for determining the liquid Twomey effect. Regionally, our analysis of the Twomey effect shows liquid activation of cloud droplets to be important near and on land and sources of pollution. The dominant parameters for the global mean cloud adjustments remain the same after constraining to the model base state, both of which appear as exponents in the autoconversion parameterization. Our results are similar to those of Gettelman et al. (2024), who also analyse a CAM6 perturbed parameter ensemble and use linear regression to identify important parameters related to ACI and find parameters in the cloud microphysics scheme, including *micro_mg_autocon_lwp_exp* to be important. Additionally, Mikkelsen et al. (2025) found that the posterior distributions of both *micro_mg_autocon_lwp_exp*, and *micro_mg_autocon_nd_exp* were constrained relative to a uniform prior when comparing to observations based off precipitation, liquid water path, and CDNC. Though a difference in posterior in comparison to a uniform prior distribution does not correspond to parameter sensitivity, it does show that these two parameters produce a variety of climates throughout the sampling space. The autoconversion parameterization controls the rain-rate in warm clouds. Altering the rain rate of clouds, is a proven mechanism for LWP and cloud fraction adjustments (Albrecht, 1989). Our analysis cements the notion that aerosol emission and activation parameters control the Twomey effect,



170 while the autoconversion parameters play a key role in how the liquid water in the cloud evolves after CDNC has been modified.

We also performed further analysis constraining a posterior distribution using PD satellite observations (see supplement). This included global mean net SW TOA flux, outgoing long-wave radiation (OLR), SW cloud radiative effect (CRE), and LWP from CERES EBAF satellite observations, (Elsaesser et al., 2025, Loeb et al., 2018, 2020). We found that these variables alone do not constrain *micro_mg_dcs* for the Twomey effect, likely due to the omission of IWP. It was found that
175 *microp_aero_npccn_scale* was the second most dominant parameter for the liquid Twomey effect after *micro_mg_dcs*, with the other dominant parameters both exponents in the autoconversion equation. For the cloud adjustments, the two most dominant parameters remained the autoconversion exponents. Thus, constraining to the observed climate state, rather than the model base state, does not qualitatively affect the results and continues to display the importance of activation-related parameters for the Twomey effect, and the autoconversion parameters for the liquid cloud adjustments.

180

4 Conclusion

PPE studies are important for understanding the effective radiative forcing of aerosol cloud interactions and quantifying the uncertainties in their representations in GCMs. Our analysis demonstrates that accounting for the PD model base state is essential when interpreting PPE output. Allowing unrealistic cloud properties can distort the assessment of parameter
185 importance and lead to incorrect conclusions about process sensitivity. By constraining to the base state, the parameter dependence in our PPE changed substantially. Under uniform prior sampling, autoconversion parameterizations for liquid and ice clouds appeared to drive the liquid cloud Twomey effect. After applying constraints on the base state, parameters related to aerosols and activation become the primary controls on the Twomey effect. In contrast, the dominant parameters for the LWP and CF adjustments, the exponents in the autoconversion parameterization, remain consistent before and after
190 rejection sampling, indicating that these adjustments are less sensitive to the model's base state. Spatially, parameter sensitivities for the Twomey effect show a regime-dependent structure where aerosol emission and activation parameters dominate over polluted land regions and background cloud water content controls the response in pristine regions. We also find that controlling for IWP is critical for isolating liquid cloud behavior, as ice clouds can obscure the sensitivity of liquid cloud processes. We note that these results are specific to CAM6 and uncertainties are introduced in the emulators used as
195 well as the choice of constraining variables; while we selected global mean LWP, IWP, TOA net SW flux, and liquid CF to represent a coherent PD cloud state, other constraints or mean climates could alter parameter importance. Despite these limitations, this analysis outlines a computationally inexpensive, model-agnostic method that can be easily adopted across all PPE output to produce more physically meaningful parameter sensitivities. Further research should address the local distribution of cloud regimes created by parameter dominance maps to understand how different regions respond to aerosol
200 across the globe.



Appendix A: Methods

A.1 PPE

Our analysis uses data from a PPE using CAM6 outlined in Duran et al., (2025a). The ensemble consists of 162 atmosphere-only simulations, where 19 aerosol and microphysics parameters are simultaneously varied using a Latin hypercube sampling technique (Eidhammer et al., 2024). Varied parameters and their respective ranges can be found in Table B1. 1 of the 162 members retains the CAM6 default parameter values: this simulation represents the base state of the model. For each ensemble member, pairs of simulations were run to represent pre-industrial (PI) and present-day (PD) climates where only the aerosol precursors and emissions are changed. PI aerosol emissions represent emissions from the year 1850 (Hoesly et al., 2018), while PD aerosol emissions are chosen to be a climatological average over the 2006–2014 period. Sea surface temperature and sea ice cover are prescribed to climatological averages over 2005–2015. Horizontal winds are nudged above the boundary layer to Modern-Era Retrospective analysis for Research Applications, Version 2 (MERRA2; Koster et al., 2015) reanalysis fields from 2010–2011. Each ensemble member outputs joint histograms of r_e and LWP for liquid-topped clouds, which serve as input to the ERFaci decomposition described in Section A.2

A.2 MODIS Cloud Radiative Kernel Decomposition

The SW ERFaci is decomposed into contributions from the Twomey effect, LWP adjustments, and CF adjustments following the method outlined in Duran et al. (2025b). This method combines the MODIS satellite instrument simulator component with a shortwave cloud radiative kernel to decompose the SW ERFaci from liquid clouds. Joint-histograms of r_e and liquid water path for liquid-topped clouds are partitioned by the MODIS satellite instrument simulator component. The RRTMG radiative transfer model (Clough et al., 2005) is used to compute the SW cloud radiative kernels. Each kernel represents the sensitivity of SW radiative flux at the TOA given by a unit increase in liquid CF for each joint-histogram bin. The SW cloud radiative kernel is linearly interpolated into latitude-longitude space to decompose the SW radiative flux anomaly at the top of the atmosphere induced by changes in liquid-topped clouds into contributions from changes in r_e , LWP, and CF. More detailed information about the method can be found in Duran et al. (2025b).

225

A.3 Emulation and Sensitivity Analysis

To constrain the parameter space to match the PD model base state, Gaussian Process (GP) emulators were built using the ESEm package (Watson-Parris et al., 2021). Output from the PPE was used as the training and testing data for each PD global mean base state variable, as well as for the global mean and local liquid cloud Twomey effect and the global mean of each macrophysical adjustment diagnosed from the MODIS CRK method. GP emulators can capture complex non-linear relationships between the parameters and the selected output and were selected by systematically choosing the best kernel and noise combination via R^2 score. Using each emulator for the predictor variables, LWP, IWP, MODIS liquid CF, and

230



TOA net SW flux over $1e9$ samples were drawn from the uniform prior parameter space. A rejection sampling technique was then applied to create a posterior cumulative distribution function for each input parameter (Eidhammer et al., 2024). The posterior distribution was formed by retaining samples in the prior input space that matched the global mean model base state across all four PD variables. Applying the posterior distribution to the emulators for the Twomey Effect, LWP and CF adjustments we were able to run a global sensitivity analysis using the PAWN method (Pianosi and Wagener, 2015, Herman and Usher 2017, Iwanaga et al., 2022). PAWN is a distribution-based global sensitivity analysis method that measures the influence of input parameters by quantifying changes in the output cumulative distribution function. PAWN produces sensitivity indices that rank parameters according to their influence on the full output distribution. Unlike linear regression, which assumes a linear relationship between inputs and outs, PAWN can learn nonlinear responses within the model. This results in indices that quantify the influence of each parameter within the physically constrained posterior parameter space. The same sensitivity analysis was also applied to the full prior distribution to allow direct comparison of parameter importance before and after the base state constraint.

B.1 Parameter Key

TABLE B1. A description of the parameters perturbed in the PPE and their ranges.

Parameter	Description	Default	Min	Max	Units
micro_mg_accre_enhan_fact	Accretion enhancing factor	1	0.1	10	–
micro_mg_autocon_fact	Autoconversion factor	0.01	5e-3	0.2	–
micro_mg_autocon_lwp_exp	KK2000 LWP exponent	2.47	1.8	3.6	–
micro_mg_autocon_nd_exp	KK2000 autoconversion factor	-1.1	-2.5	0	–
micro_mg_berg_eff_factor	Bergeron efficiency factor	1	0.1	1	–
micro_mg_dcs	Autoconversion size threshold ice-snow	5e-4	5e-5	1e-3	m
micro_mg_effi_factor	Scale effective radius for optics calculation	1	0.1	2	–
micro_mg_homog_size	Homogeneous freezing ice particle size	2.5e-5	1e-5	2e-4	m
micro_mg_iaccr_factor	Scaling ice/snow accretion	1	0.2	1	–
micro_mg_max_nicons	Max ice number concentration	1e8	1e5	1e10	# kg ⁻¹
micro_mg_vtrmi_factor	Ice fall speed scaling	1	0.2	5	m s ⁻¹
seasalt_emis_scale	Sea salt emission scaling factor	1	0.5	2.5	–
microp_aero_npccn_scale	Scale activated liquid number	1	0.33	3	–
microp_aero_wsub_min	Min sub grid velocity for liquid activation	0.2	0	0.5	m s ⁻¹
microp_aero_wsubi_min	Min sub grid velocity for ice activation	1e-3	0	0.2	m s ⁻¹
microp_aero_wsub_scale	Sub grid cell velocity for liquid activation scaling	1	0.1	5	–
microp_aero_wsubi_scale	Sub grid cell velocity for ice activation scaling	1	0.1	5	–
dust_emis_fact	Dust emissions scaling factor	0.7	0.1	1.2	–
sol_facti_cloud_borne	In-cloud scavenging of cloud-borne modal aerosols	1	0.5	1	–



250 **Author contributions**

S.W. conducted data analysis and wrote the first draft of the manuscript. B.M.D. designed and performed the perturbed parameter ensemble simulations and decomposition. S.W., D.W.P. and J.M. designed research methodology. All authors contributed to revising and editing the final manuscript.

Competing interests

255 At least one of the (co-)authors is a member of the editorial board of Atmospheric Chemistry and Physics.

Acknowledgements

We greatly wish to thank Gregory Elsaesser for sharing the post-processed CERES EBAF satellite observations, used in Elsaesser et al., 2025. D.W.P and S.W. acknowledge funding from U.S. National Science Foundation award 2441832.

B.M.D. is supported by the National Science Foundation Graduate Research Fellowship under Grant No. DGE-2038238.

260 The authors would like to acknowledge high-performance computing support from the Derecho system (doi:10.5065/qx9a-pg09) provided by the NSF National Center for Atmospheric Research (NCAR), sponsored by the National Science Foundation.

265 **Data Availability**

Monthly data from the PPE used in this study are available on the NSF NCAR Derecho system and all relevant variables to this study will be made publicly available on Zenodo upon publication of the manuscript.

270

275

280

285

290



References

- 295 Ackerman, A. S., Kirkpatrick, M. P., Stevens, D. E., and Toon, O. B.: The impact of humidity above stratiform clouds on indirect aerosol climate forcing, *Nature*, 432, 1014–1017, <https://doi.org/10.1038/nature03174>, 2004.
- Albrecht, B. A.: Aerosols, Cloud Microphysics, and Fractional Cloudiness, *Science*, 245, 1227–1230, <https://doi.org/10.1126/science.245.4923.1227>, 1989.
- 300 Bellouin, N., Quaas, J., Gryspeerdt, E., Kinne, S., Stier, P., Watson-Parris, D., Boucher, O., Carslaw, K. S., Christensen, M., Daniau, A. -L., Dufresne, J. -L., Feingold, G., Fiedler, S., Forster, P., Gettelman, A., Haywood, J. M., Lohmann, U., Malavelle, F., Mauritsen, T., McCoy, D. T., Myhre, G., Mülmenstädt, J., Neubauer, D., Possner, A., Rugenstein, M., Sato, Y., Schulz, M., Schwartz, S. E., Sourdeval, O., Storelvmo, T., Toll, V., Winker, D., and Stevens, B.: Bounding Global Aerosol Radiative Forcing of Climate Change, *Reviews of Geophysics*, 58, e2019RG000660, <https://doi.org/10.1029/2019RG000660>, 2020.
- 305 Bhatti, Y. A., Watson-Parris, D., Regayre, L. A., Jia, H., Neubauer, D., Im, U., Svenhag, C., Schutgens, N., Tsikerdekis, A., Nenes, A., Irfan, M., van Dienenhoven, B., Arifi, A., Fu, G., and Hasekamp, O. P.: Uncertainty in aerosol effective radiative forcing from anthropogenic and natural aerosol parameters in ECHAM6.3-HAM2.3, *Atmospheric Chemistry and Physics*, 26, 269–293, <https://doi.org/10.5194/acp-26-269-2026>, 2026.
- 310 Bretherton, C. S., Blossey, P. N., and Uchida, J.: Cloud droplet sedimentation, entrainment efficiency, and subtropical stratocumulus albedo, *Geophysical Research Letters*, 34, <https://doi.org/10.1029/2006GL027648>, 2007.
- 315 Carslaw, K. S., Lee, L. A., Reddington, C. L., Pringle, K. J., Rap, A., Forster, P. M., Mann, G. W., Spracklen, D. V., Woodhouse, M. T., Regayre, L. A., and Pierce, J. R.: Large contribution of natural aerosols to uncertainty in indirect forcing, *Nature*, 503, 67–71, <https://doi.org/10.1038/nature12674>, 2013.
- Chen, Y.-C., Christensen, M. W., Stephens, G. L., and Seinfeld, J. H.: Satellite-based estimate of global aerosol–cloud radiative forcing by marine warm clouds, *Nature Geosci*, 7, 643–646, <https://doi.org/10.1038/ngeo2214>, 2014.
- 320 Clough, S. A., Shephard, M. W., Mlawer, E. J., Delamere, J. S., Iacono, M. J., Cady-Pereira, K., Boukabara, S., and Brown, P. D.: Atmospheric radiative transfer modeling: a summary of the AER codes, *Journal of Quantitative Spectroscopy and Radiative Transfer*, 91, 233–244, <https://doi.org/10.1016/j.jqsrt.2004.05.058>, 2005.
- 325 Douglas, A. and L’Ecuyer, T.: Quantifying variations in shortwave aerosol–cloud–radiation interactions using local meteorology and cloud state constraints, *Atmospheric Chemistry and Physics*, 19, 6251–6268, <https://doi.org/10.5194/acp-19-6251-2019>, 2019.
- 330 Duran, B. M., Lutsko, N. J., and Wall, C. J.: Aerosol-Ice-Cloud Interactions in a Perturbed Parameter Ensemble, *Authorea* [preprint], <https://doi.org/10.22541/au.176599461.12824917/v1>, 2025a.
- Duran, B. M., Wall, C. J., Lutsko, N. J., Michibata, T., Ma, P.-L., Qin, Y., Duffy, M. L., Medeiros, B., and Debolskiy, M.: A new method for diagnosing effective radiative forcing from aerosol–cloud interactions in climate models, *Atmospheric Chemistry and Physics*, 25, 2123–2146, <https://doi.org/10.5194/acp-25-2123-2025>, 2025b.
- 335 Eidhammer, T., Gettelman, A., Thayer-Calder, K., Watson-Parris, D., Elsaesser, G., Morrison, H., van Lier-Walqui, M., Song, C., and McCoy, D.: An extensible perturbed parameter ensemble for the Community Atmosphere Model version 6, *Geoscientific Model Development*, 17, 7835–7853, <https://doi.org/10.5194/gmd-17-7835-2024>, 2024.



- 340 Elsaesser, G. S., van Lier-Walqui, M., Yang, Q., Kelley, M., Ackerman, A. S., Fridlind, A. M., Cesana, G. V., Schmidt, G. A., Wu, J., Behrangi, A., Camargo, S. J., De, B., Inoue, K., Leitmann-Niimi, N. M., and Strong, J. D. O.: Using Machine Learning to Generate a GISS ModelE Calibrated Physics Ensemble (CPE), *Journal of Advances in Modeling Earth Systems*, 17, e2024MS004713, <https://doi.org/10.1029/2024MS004713>, 2025.
- 345 Gettelman, A., Eidhammer, T., Duffy, M. L., McCoy, D. T., Song, C., and Watson-Parris, D.: The Interaction Between Climate Forcing and Feedbacks, *Journal of Geophysical Research: Atmospheres*, 129, e2024JD040857, <https://doi.org/10.1029/2024JD040857>, 2024.
- 350 Gryspeerdt, E., Quaas, J., Ferrachat, S., Gettelman, A., Ghan, S., Lohmann, U., Morrison, H., Neubauer, D., Partridge, D. G., Stier, P., Takemura, T., Wang, H., Wang, M., and Zhang, K.: Constraining the instantaneous aerosol influence on cloud albedo, *Proceedings of the National Academy of Sciences*, 114, 4899–4904, <https://doi.org/10.1073/pnas.1617765114>, 2017.
- Herman, J. and Usher, W.: SALib: An open-source Python library for Sensitivity Analysis, *Journal of Open Source Software*, 2, 97, <https://doi.org/10.21105/joss.00097>, 2017.
- 355 Hoesly, R. M., Smith, S. J., Feng, L., Klimont, Z., Janssens-Maenhout, G., Pitkanen, T., Seibert, J. J., Vu, L., Andres, R. J., Bolt, R. M., Bond, T. C., Dawidowski, L., Kholod, N., Kurokawa, J., Li, M., Liu, L., Lu, Z., Moura, M. C. P., O'Rourke, P. R., and Zhang, Q.: Historical (1750–2014) anthropogenic emissions of reactive gases and aerosols from the Community Emissions Data System (CEDS), *Geoscientific Model Development*, 11, 369–408, <https://doi.org/10.5194/gmd-11-369-2018>, 2018.
- 360 Iwanaga, T., Usher, W., and Herman, J.: Toward SALib 2.0: Advancing the accessibility and interpretability of global sensitivity analyses, *Socio-Environmental Systems Modelling*, 4, 18155–18155, <https://doi.org/10.18174/sesmo.18155>, 2022.
- 365 Khairoutdinov, M. and Kogan, Y.: A New Cloud Physics Parameterization in a Large-Eddy Simulation Model of Marine Stratocumulus, *10 Mon. Wea. Rev.*, 128, 229—243, 2000
- 370 Koster, R. D., Bosilovich, M. G., Akella, S., Lawrence, C., Cullather, R., Draper, C., Gelaro, R., Kovach, R., Liu, Q., Molod, A., Norris, P., Wargan, K., Chao, W., Reichle, R., Takacs, L., Todling, R., Vikhliayev, Y., Bloom, S., Collow, A., Partyka, G., Labow, G., Pawson, S., Reale, O., Schubert, S., and Suarez, M.: Technical Report Series on Global Modeling and Data Assimilation, Volume 43: Initial Evaluation of the Climate - MERRA-2, 2015.
- 375 Lee, L. A., Carslaw, K. S., Pringle, K. J., Mann, G. W., and Spracklen, D. V.: Emulation of a complex global aerosol model to quantify sensitivity to uncertain parameters, *Atmos. Chem. Phys.*, 11, 12253–12273, <https://doi.org/10.5194/acp-11-12253-2011>, 2011.
- 380 Lee, L. A., Pringle, K. J., Reddington, C. L., Mann, G. W., Stier, P., Spracklen, D. V., Pierce, J. R., and Carslaw, K. S.: The magnitude and causes of uncertainty in global model simulations of cloud condensation nuclei, *Atmos. Chem. Phys.*, 13, 8879–8914, <https://doi.org/10.5194/acp-13-8879-2013>, 2013.
- 385 Loeb, N. G., Doelling, D. R., Wang, H., Su, W., Nguyen, C., Corbett, J. G., Liang, L., Mitrescu, C., Rose, F. G., and Kato, S.: Clouds and the Earth's Radiant Energy System (CERES) Energy Balanced and Filled (EBAF) top-of-atmosphere (TOA) Edition-4.0 data product, *J. Climate*, 31, 895–918, <https://doi.org/10.1175/JCLI-D-17-0208.1>, 2018.
- Loeb, N. G., Rose, F. G., Kato, S., Rutan, D. A., Su, W., Wang, H., Doelling, D. R., Smith, W. L., and Gettelman, A.: Toward a Consistent Definition between Satellite and Model Clear-Sky Radiative Fluxes, *J. Climate*, 33, 61–75, <https://doi.org/10.1175/JCLI-D-19-0381.1>, 2020.



- 390 Mikkelsen, A., McCoy, D. T., Eidhammer, T., Gettelman, A., Song, C., Gordon, H., and McCoy, I. L.: Constraining aerosol–cloud adjustments by uniting surface observations with a perturbed parameter ensemble, *Atmospheric Chemistry and Physics*, 25, 4547–4570, <https://doi.org/10.5194/acp-25-4547-2025>, 2025.
- 395 Morrison, H. and Gettelman, A.: A New Two-Moment Bulk Stratiform Cloud Microphysics Scheme in the Community Atmosphere Model, Version 3 (CAM3). Part I: Description and Numerical Tests, *J Climate*, 21, 3642–3659, <https://doi.org/10.1175/2008JCLI2105.1>, 2008.
- 400 Morrison, H., van Lier-Walqui, M., Fridlind, A. M., Grabowski, W. W., Harrington, J. Y., Hoose, C., Korolev, A., Kumjian, M. R., Milbrandt, J. A., Pawlowska, H., Posselt, D. J., Prat, O. P., Reimel, K. J., Shima, S.-I., van Dienenhoven, B., and Xue, L.: Confronting the Challenge of Modeling Cloud and Precipitation Microphysics, *Journal of Advances in Modeling Earth Systems*, 12, e2019MS001689, <https://doi.org/10.1029/2019MS001689>, 2020.
- 405 Mülmenstädt, J. and Feingold, G.: The Radiative Forcing of Aerosol–Cloud Interactions in Liquid Clouds: Wrestling and Embracing Uncertainty, *Curr Clim Change Rep*, 4, 23–40, <https://doi.org/10.1007/s40641-018-0089-y>, 2018.
- Mülmenstädt, J., Nam, C., Salzmann, M., Kretzschmar, J., L’Ecuyer, T. S., Lohmann, U., Ma, P.-L., Myhre, G., Neubauer, D., Stier, P., Suzuki, K., Wang, M., and Quaas, J.: Reducing the aerosol forcing uncertainty using observational constraints on warm rain processes, *Science Advances*, 6, eaaz6433, <https://doi.org/10.1126/sciadv.aaz6433>, 2020.
- 410 Pianosi, F. and Wagener, T.: A simple and efficient method for global sensitivity analysis based on cumulative distribution functions, *Environmental Modelling & Software*, 67, 1–11, <https://doi.org/10.1016/j.envsoft.2015.01.004>, 2015.
- 415 Quaas, J., Ming, Y., Menon, S., Takemura, T., Wang, M., Penner, J. E., Gettelman, A., Lohmann, U., Bellouin, N., Boucher, O., Sayer, A. M., Thomas, G. E., McComiskey, A., Feingold, G., Hoose, C., Kristjánsson, J. E., Liu, X., Balkanski, Y., Donner, L. J., Ginoux, P. A., Stier, P., Grandey, B., Feichter, J., Sednev, I., Bauer, S. E., Koch, D., Grainger, R. G., Kirkevåg, A., Iversen, T., Seland, Ø., Easter, R., Ghan, S. J., Rasch, P. J., Morrison, H., Lamarque, J.-F., Iacono, M. J., Kinne, S., and Schulz, M.: Aerosol indirect effects – general circulation model intercomparison and evaluation with satellite data, *Atmospheric Chemistry and Physics*, 9, 8697–8717, <https://doi.org/10.5194/acp-9-8697-2009>, 2009.
- 420 Regayre, L. A., Johnson, J. S., Yoshioka, M., Pringle, K. J., Sexton, D. M. H., Booth, B. B. B., Lee, L. A., Bellouin, N., and Carslaw, K. S.: Aerosol and physical atmosphere model parameters are both important sources of uncertainty in aerosol ERF, *Atmos. Chem. Phys.*, 18, 9975–10006, <https://doi.org/10.5194/acp-18-9975-2018>, 2018.
- 425 Seinfeld, J. H., Bretherton, C., Carslaw, K. S., Coe, H., DeMott, P. J., Dunlea, E. J., Feingold, G., Ghan, S., Guenther, A. B., Kahn, R., Kraucunas, I., Kreidenweis, S. M., Molina, M. J., Nenes, A., Penner, J. E., Prather, K. A., Ramanathan, V., Ramaswamy, V., Rasch, P. J., Ravishankara, A. R., Rosenfeld, D., Stephens, G., and Wood, R.: Improving our fundamental understanding of the role of aerosol–cloud interactions in the climate system, *Proc. Natl. Acad. Sci. U.S.A.*, 113, 5781–5790, <https://doi.org/10.1073/pnas.1514043113>, 2016.
- 430 Song, C., McCoy, D. T., Eidhammer, T., Gettelman, A., McCoy, I. L., Watson-Parris, D., Wall, C. J., Elsaesser, G., and Wood, R.: Buffering of Aerosol-Cloud Adjustments by Coupling Between Radiative Susceptibility and Precipitation Efficiency, *Geophysical Research Letters*, 51, e2024GL108663, <https://doi.org/10.1029/2024GL108663>, 2024.
- 435 Twomey, S.: *The Influence of Pollution on the Shortwave Albedo of Clouds*, 1977.
- Wall, C. J., Norris, J. R., Possner, A., McCoy, D. T., McCoy, I. L., and Lutsko, N. J.: Assessing effective radiative forcing from aerosol–cloud interactions over the global ocean, *Proceedings of the National Academy of Sciences*, 119, e2210481119, <https://doi.org/10.1073/pnas.2210481119>, 2022.



- 440 Wang, S., Wang, Q., and Feingold, G.: Turbulence, Condensation, and Liquid Water Transport in Numerically Simulated Nonprecipitating Stratocumulus Clouds, *J. Atmos. Sci.*, **60**, 262–278, [https://doi.org/10.1175/1520-0469\(2003\)060<0262:TCALWT>2.0.CO;2](https://doi.org/10.1175/1520-0469(2003)060<0262:TCALWT>2.0.CO;2). 2003.
- 445 Watson-Parris, D.: Integrating Top-Down Energetic Constraints With Bottom-Up Process-Based Constraints for More Accurate Projections of Future Warming, *Geophysical Research Letters*, 52, e2024GL114269, <https://doi.org/10.1029/2024GL114269>, 2025.
- 450 Watson-Parris, D., Williams, A., Deaconu, L., and Stier, P.: Model calibration using ESEm v1.1.0 – an open, scalable Earth system emulator, *Geoscientific Model Development*, 14, 7659–7672, <https://doi.org/10.5194/gmd-14-7659-2021>, 2021.
- Yang, Q., Elsaesser, G. S., van Lier-Walqui, M., and Eidhammer, T.: A Simple Emulator That Enables Interpretation of Parameter-Output Relationships, Applied to Two Climate Model PPEs, *Journal of Advances in Modeling Earth Systems*, 17, e2024MS004766, <https://doi.org/10.1029/2024MS004766>, 2025.